Volume 214 • Number 23 • December 12, 2013

www.mcp-journal.de

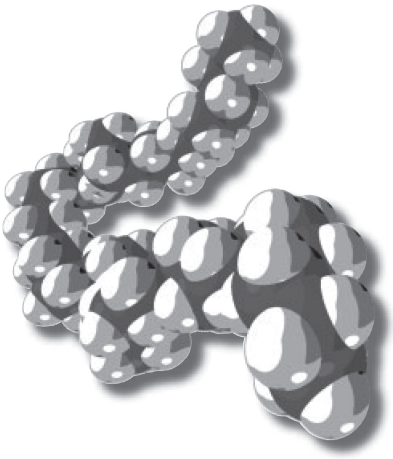

Macromolecular Chemistry and Physics

Founded by
Hermann Staudinger

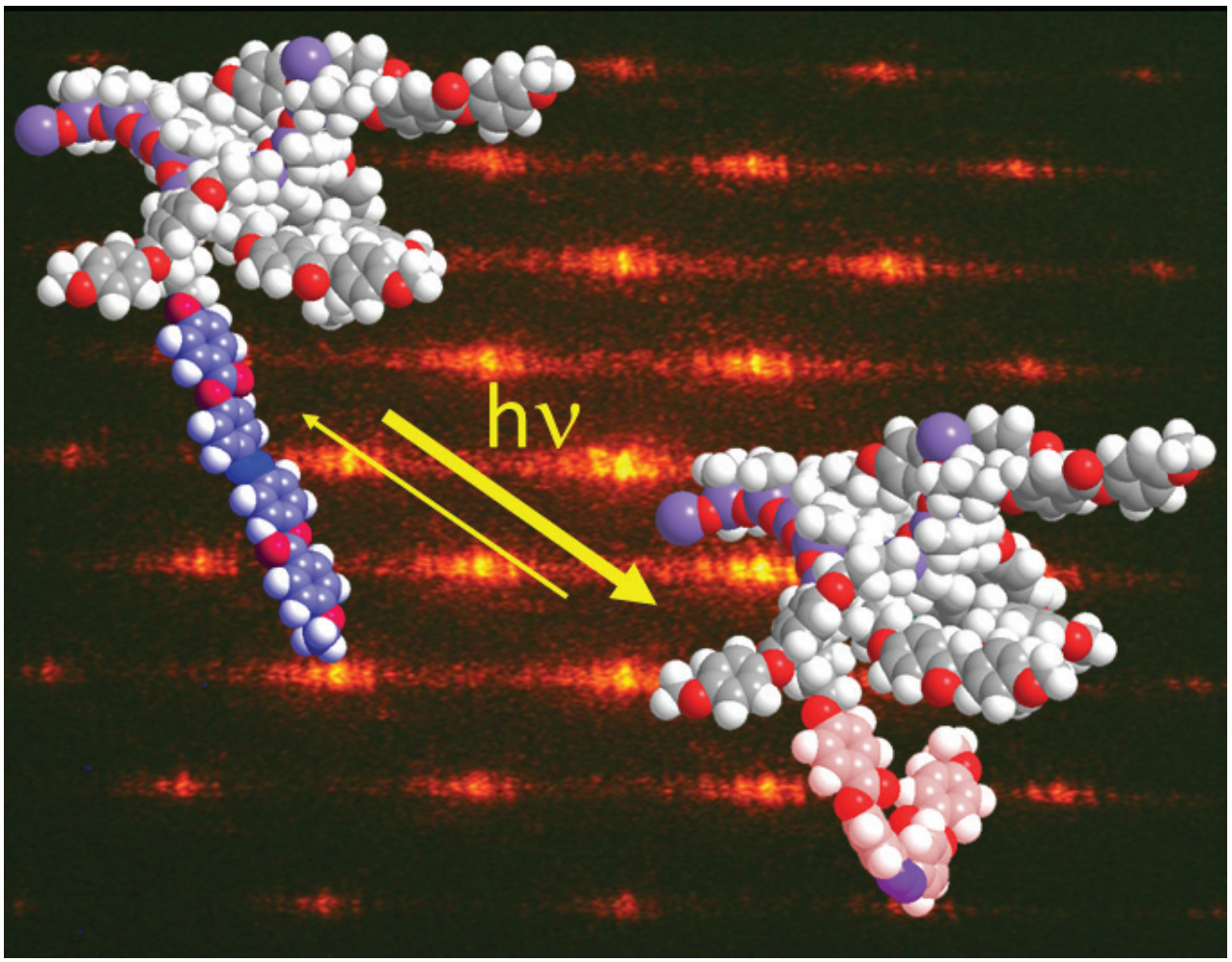

23/2013

WILEY-VCH

Light-Induced Refractive Index Modulation in Photoactive Liquid-Crystalline Elastomers

Blaž Tašič, Wei Li, Antoni Sánchez-Ferrer, Martin Čopič, Irena Drevenšek-Olenik*

A comparative study of UV-irradiation-induced refractive index modulation in two analogous monodomain nematic side-chain liquid-crystalline elastomer materials is conveyed. In one of them, mesogenic azobenzene derivatives are incorporated as pendant co-monomers, and in the other as crosslinking units. The dependence of the optical diffraction properties on the polarization state of the probe beam reveals that diffraction is predominantly of a bulk origin for both materials. For prolonged UV exposures, the material with pendant azobenzene derivatives exhibits practically constant diffraction properties, while the material with cross-linking azobenzene units shows a profound decrease of diffraction efficiency with increasing exposure time. The difference is attributed to photoinduced alignment of the azobenzene molecules, which is much stronger in the material with the crosslinking azobenzene units.

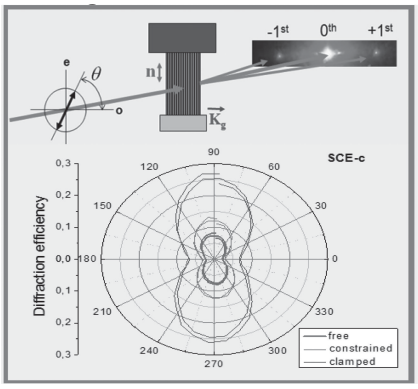

1. Introduction

Adding a small amount of photoactive component to the polymer matrix opens up different possibilities for optical manipulation of mechanical, thermal, electrical, and optical properties of the polymeric material.[1–4] Recently, light-induced phenomena in liquid-crystalline elastomers (LCEs) containing photoisomerizable azobenzene derivatives has gained a lot of attention. This type of LCE exhibits very interesting opto-mechanical properties that are a direct consequence of the coupling mechanism between conformational state of the polymer chains and orientational order of the liquid-crystalline molecules (mesogens), which depends on the isomerization state of the azobenzene molecules.[5–7] If exposed to optical irradiation, they change their size and shape, flip between different shapes, oscillate, or even move on the supporting surface.[8–15] This makes them very promising for photomechanical transducers, actuators, cantilevers, microfluidic tools, etc.[16–23] Another interesting property of azo-containing LCEs is their huge opto-optical response, which is associated with huge light-induced modifications of the optical refractive index, that appear due to collective response of the LCE medium to the *trans*-to-*cis* photoisomerization process. For that reason optical patterning of LCEs provides simple fabrication of tunable optical diffraction structures (volume holograms) that can easily be manipulated by external strain and/or temperature variations.[24–26]

A photoactive moiety can be incorporated into the LCE matrix by different methods: for example, physically dissolved in the network via a swelling process or chemically attached to different segments of the material

B. Tašič, Prof. M. Čopič, Prof. I. Drevenšek-Olenik
Faculty of Mathematics and Physics, University of Ljubljana, Jadranska 19, 1000 Ljubljana, Slovenia, J. Stefan Institute, Jamova 39, SI1000, Ljubljana, Slovenia
E-mail: irena.drevensek@ijs.si
Dr. W. Li
Nankai University, TEDA APS, 23 Hongda Street, Tianjin 300457, PR China
Dr. A. Sánchez-Ferrer
Department of Health Sciences and Technology, ETH Zurich, Schmelzbergstrasse 9, 8091 Zurich, Switzerland

DOI: 10.1002/macp.201300493

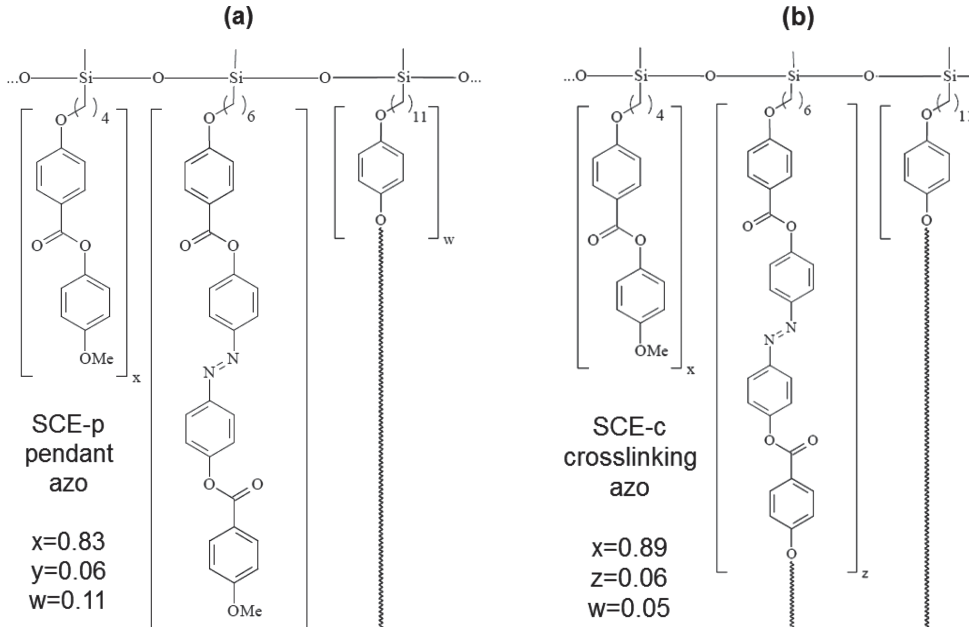

Figure 1. Chemical structure of the LCE materials SCE-p (a) and SCE-c (b).

structure.[27–29] In our recent paper, it was shown that two different means of chemical incorporation of azobenzene derivatives into a monodomain of a nematic side-chain liquid-crystalline elastomer (SC-LCE), namely as pendant co-monomer groups or as crosslinking units, resulted in a profound difference of their opto-mechanical response.[28] In this paper, we report on a comparative study of opto-optical response of the same two types of the LCE materials. We show that, in contrast to opto-mechanical efficiency, the opto-optical efficiency is considerably larger for the material including azobenzene moiety as a pendant group. The difference is explained by a mismatch between direct shape modifications related to conformational conversion of the azobenzene moiety (*trans*-to-*cis* "shrinking") and indirect shape modifications related to photoisomerization-induced decrease of the nematic liquid-crystalline order. This mismatch is predominant in the material with the crosslinking azobenzene units.

2. Experimental Section

The synthesis of poly(methylhydrosiloxane)-based nematic side-chain LCE materials denoted as SCE-p (pendant azobenzene monomer, Figure 1a and SCE-c (crosslinking azobenzene monomer, Figure 1b) is described elsewhere.[28] Aligned monodomain films with a thickness of about 300 μm were prepared according to the two-step "Finkelmann crosslinking procedure."[30] Both materials contain the same fraction of azoderivative (5.6 mol%) and the same concentration of crosslinker (11.1 mol%), and exhibit a glass transition temperature (T_g) below room temperature. Their absorption maxima related to all *trans*-conformation of the azo-derivatives appear at λ_{ab} = 358 ± 1 nm. Figure 2 shows results of analysis of spontaneous thermal contraction of both materials in absence of UV illumination. The contraction takes place along the direction of the nematic director **n**. From the obtained dependencies, one can deduce that the nematic-paranematic phase transition of SCE-p and SCE-c occurs at $T_{c\text{-}p} \approx 82$ °C and $T_{c\text{-}c} \approx 110$ °C, respectively. The higher T_c value for SCE-c is associated with its larger concentration of mesogenic molecular groups (88.8 mol% for SCE-c versus 83.3 mol% for SCE-p). However, at room temperature, both materials exhibit quite similar liquid-crystalline order.[28]

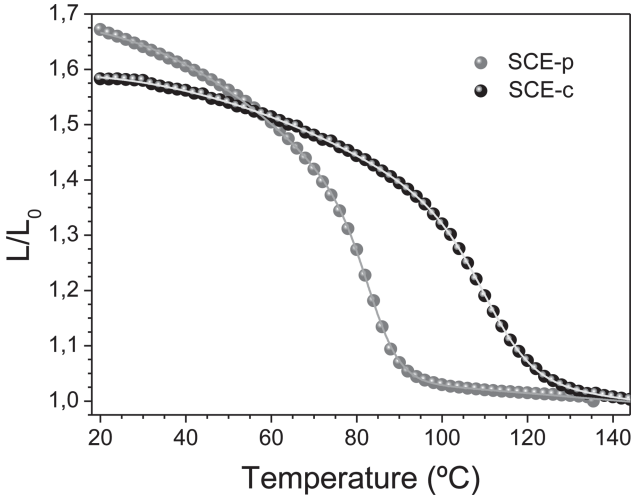

Figure 2. Temperature dependence of normalized sample length *L* along the direction of nematic director **n**, where L_o denotes length at the highest temperature applied in our experiment.

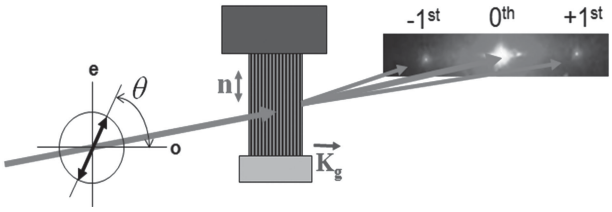

Figure 3. Experimental setup for the analysis of optical diffraction properties. Vectors **n** and $\boldsymbol{K}_g$ denote nematic director and optical grating vector, respectively. Azimuthal angle θ denotes polarization direction of the probe beam, where θ = o corresponds to ordinary (o) and $\theta = 90°$ to extraordinary (e) polarization. Image on the right shows diffraction peaks observed on a white screen placed 20 cm behind the sample. The bright spot marked as 0th order peak corresponds to the transmitted beam and the spots marked as ±1st order peaks correspond to diffracted beams.

Optical experiments were performed at room temperature (≈296 K). Films of the size of 5 mm × 2 mm were mounted into the setup in three different configurations. In the "free" configuration, the upper edge of the film was fixed to the frame of the sample holder, while the lower edge was hanging freely in the air, loaded only with a small weight of 0.5 g. In the "clamped" configuration both, the upper and the lower edge of the film, were fixed to the frame and before starting the experiments the film was stretched for 10% of its natural length. In these two cases, the nematic director **n** was parallel to the direction of external stress. In the "constrained" configuration, the film was placed between two glass plates that were pressed together with a constant force. Surface friction constrained size modifications of the sample in the plane of the plates. In this configuration, external stress was perpendicular to the nematic director **n**.

The samples were irradiated with an interference field of two intersecting UV laser beams from an Argon ion laser operating at a recording wavelength of $\lambda_R = 351$ nm. The beams were expanded to the cross-section of about 0.2 cm^2. The power of each UV beam impinging on the sample was 10 mW. The intersection angle between the beams was 1.1° resulting in an optical interference pattern with periodicity $\Lambda = 9.3$ μm. UV irradiation stimulates photoisomerization of the azobenzene moiety and this causes modification of the material refractive index. The rate of isomerization process is proportional to the UV intensity. Accordingly, illumination with the periodic intensity pattern results in formation of a 1D optical transmission grating with grating period Λ. In our experiments, the grating vector $\boldsymbol{K}_g = (2\pi/\Lambda)\boldsymbol{e}_g$ was perpendicular to the nematic director **n**. The polarization of the UV beams was parallel to **n** (i.e., the beams were extraordinarily (e) polarized).

Optical diffraction efficiency of the recorded gratings was probed with a low-power (<1 mW) beam from a He–Ne laser operating at a wavelength of $\lambda_P = 632.8$ nm. The arrangement of the probe beam is shown in Figure 3. The linearly polarized probe beam entered the film at normal incidence. In the measurements performed during UV illumination, the probe beam was extraordinarily polarized (e), while in the investigations of polarization dependence its polarization direction was rotated from ordinary (o, $\theta = 0°$) to extraordinary (e, $\theta = 90°$) using a $\lambda/2$ plate. The diameter of the probe beam in the sample was about 0.2 mm. The intensities of the 0th (transmission direction) and ±1st order diffraction peaks were detected with photodiodes. The total intensity of all higher order diffraction peaks was always below 20% of the sum of intensities of the 0th and the ±1st order peaks, so their contribution was neglected. After each experiment, the sample was heated to the paranematic phase ($T > T_c$) and slowly cooled back to room temperature to ensure full erasure of the previously formed grating structure before starting the next measurement.

Details of the mechanism of UV light-induced periodic modifications of the refractive index in azo-doped LCE films are described in our previous papers.[31,32] The modifications are in the range $\Delta n \approx 10^{-2}$, while the modulation depth is in the range of few micrometers to few tens of micrometers. Therefore, the corresponding diffraction regime for the probe beam typically lies somewhere between the thin grating (Raman–Nath) and the intermediate grating regime.[31] All of the measurements were performed at room temperature (23 °C). At this temperature, the spontaneous *cis-trans* relaxation, which causes exponential decay of the diffraction efficiency after termination of the UV irradiation, is very slow (relaxation time larger than 2 h), so its effects were neglected.[28,31]

3. Results and Discussion

3.1. Kinetics of Grating Formation

At the beginning of the illumination with the UV intensity pattern, the photoisomerization reaction takes place only in a few micrometers thick surface layer of the film, but later on, photobleaching of the azobenzene dye molecules allows UV light to penetrate deeper and deeper into the sample depth.[32,33] The associated periodic refractive index modulation causes optical diffraction of the probe beam. The kinetics of the build-up of the modulation pattern can be monitored by in situ analysis of diffraction. In our experiments, we monitored the diffraction efficiency of the 1st order diffraction peak defined as:

$$\eta = I_{+1}/(I_{+1} + I_0 + I_{-1}) \quad (1)$$

This definition of η was chosen to account for partial absorption (≈50%) of the probe beam that takes place mainly in the non-perturbed part of the LCE film. Measurements were repeated three times for each sample and each configuration.

Typical dependencies of $\eta(t)$ obtained for the material with pendant azobenzene groups (SCE-p) are shown in Figure 4. UV illumination starts at $t = 0$. The initial increase rate $(d\eta/dt) \approx 0.33$ min^{-1} is very similar for all three mounting configurations. The maximum of η is reached within few minutes from the start of the UV exposure with $0.3 < \eta_{max} < 0.4$. This is in the range of maximal possible diffraction efficiency of 0.34 for the

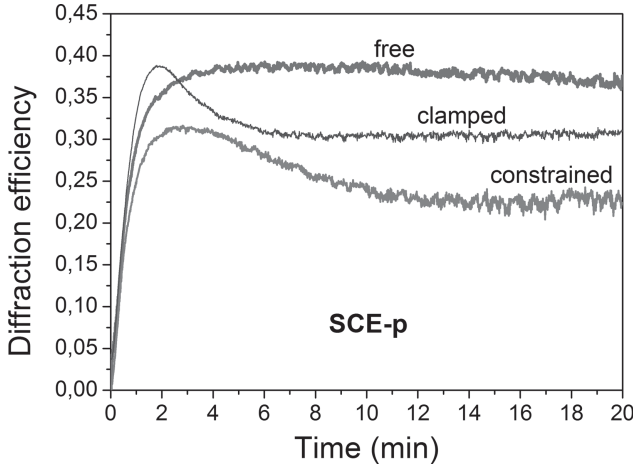

Figure 4. Time dependence of diffraction efficiency for the +1st order diffraction peak during grating formation in the material with pendant azobenzene molecules (SCE-p). The different colours/line thicknesses correspond to different mounting arrangements of the sample.

thin grating (Raman-Nath) diffraction regime.[34] For prolonged UV exposures, the effective grating depth increases approximately logarithmically with t,[32] so also phase modulation of the probe beam is expected to increase monotonously with time. However, further increase of phase modulation leads to a gradual decrease of the ±1st order diffraction intensity on behalf of the higher order diffraction peaks (over-modulation effect).[34]

Figure 5 shows results of analogous measurements for the material with the crosslinking azobenzene units (SCE-c). One can immediately notice some profound differences with respect to the material with pendant azobenzene

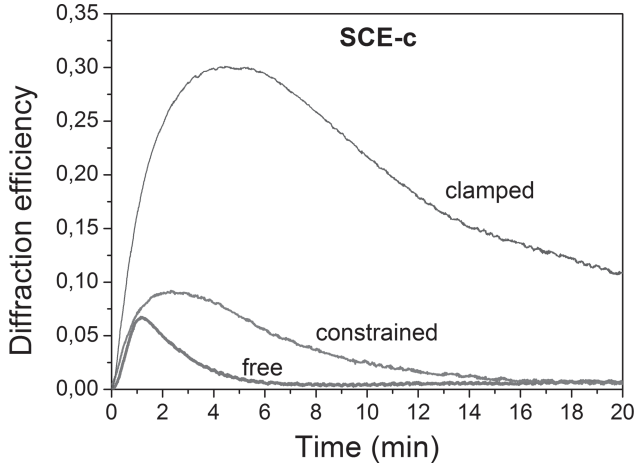

Figure 5. Time dependence of diffraction efficiency for the +1st order diffraction peak during grating formation in the material with crosslinking azobenzene units (SCE-c). Different colours/line thicknesses correspond to different mounting arrangements of the sample.

molecules. First of all, the values of η_{max} for "free" and "constrained" configurations are profoundly smaller ($\eta_{max} < 0.1$) than for the SCE-p sample ($\eta_{max} > 0.3$). In addition to this, for longer UV exposure times, the diffraction efficiency for all configurations decreases towards zero. This decrease cannot be attributed to over-modulation, because observed maximal values of η_{max}, in particular for the "free" and the "constrained" configuration, are far below the theoretically expected value of 0.34.[34] Similarly, it cannot be attributed to vibrations in the experimental setup, which are a common cause of smearing of the recorded patterns for prolonged recording times, because the same setup should then produce very similar smearing effects for both types of the samples. Hence, we believe that this decrease occurs because of a specific structural rearrangement in the SCE-c material.

In the nematic phase of the monodomain LCE, rod-shaped *trans*-azobenzene moieties are oriented predominantly along the nematic director **n**. Illumination with UV light that is linearly polarized along **n**, causes *trans*-to-*cis* photoisomerization of the azobenzene units. *Cis*-isomers act as impurities in the liquid-crystalline phase and consequently they generate a decrease of the liquid-crystalline orientational order parameter S ($S = <(3\cos^2\phi - 1)/2>$, where ϕ is the angle between the long axis of the mesogenic molecules and n and brackets denote averaging) in their neighborhood. Due to the coupling between the orientational order and the conformation of polymer chains, the decrease of S results in spontaneous contraction of the polymer network in the direction of **n**. The relation between LCE length L (in direction of **n**) and S is given by: $((L/L_0) - 1) = aS$, where L_0 is sample length at $T >> T_c$ and a is positive constant.[5] Consequently, the relative contraction can be expressed as:

$$\frac{\Delta L_s}{L} = \frac{\Delta S}{a + S} \leq \frac{\Delta S}{S} \qquad (2)$$

where ΔS is customarily explained by the down-shift of the nematic-paranematic transition temperature T_c due to the presence of the *cis* "impurities."[6,8] This effect appears in both SCE-p and SCE-c material. For temperatures far below the T_c, as is the case in our experiments, typical UV irradiation-induced modifications are in the range $(\Delta S/S) \leq 0.05$.[28,35]

Besides the contraction related to ΔS, in the SCE-c, there exists also a direct contraction of the network due to *trans*-to-*cis* isomerization. This arises because the bent-like *cis*-isomer exhibits an effective length l_c that is about 30% smaller than the effective length for the rod-like *trans*-isomer l_t.[28,36] The effective length is here considered to be a distance between the two hydrocarbon end-groups of the molecule. When such a derivative is incorporated into the LCE material as a crosslinking unit

(aligned along **n**), the isomerization process is expected to cause a local contraction of the polymer network along the direction of **n** in the range:

$$\frac{\Delta L_d}{L} = \left(\frac{\Delta l}{l_t}\right)\sqrt[3]{c_A} \quad (3)$$

where $\Delta l = l_t - l_c$ and c_A is volume fraction of the azomesogens. If, as a rough estimate for our material, we take $c_A \approx 0.05$, Equation 3 gives $\Delta L_d/L \approx 0.1$, which is considerably larger than the contraction related to $\Delta S/S$. This explains why UV illumination-induced mechanical stress, investigated in our previous paper,[28] is much larger in the SCE-c than in the SCE-p. Besides this, the above calculation also reveals that UV illumination of the LCE-c drives the material to a length modification, which is not in balance with the length modification imposed by the associated variation of the nematic order. We believe that this strongly non-equilibrium situation leads to structural rearrangements, which produce a decrease of the refractive index modulation. Consequently also the diffraction efficiency decreases.

One of the possible rearrangements that can explain the observed properties is illumination-induced contraction of the LCE film along the direction of **n**. In the "free" mounting arrangement, this causes extension of the grating structure in the direction of grating vector $\boldsymbol{K_g}$ (see Figure 3) and consequently a smearing of the recorded pattern due to motion of the material during the recording process can appear.[31] However, this effect is expected to be present only in the "free" configuration, while we observed it also in the "clamped" and "constrained" configurations.

Another rearrangement that can come into play is reorientation of the *trans*-isomers into a direction perpendicular to the direction of the UV light polarization. This photoinduced alignment is frequently observed in azobenzene-doped polymeric materials after several consecutive *trans*-to-*cis* and *cis*-to-*trans* isomerization processes and is associated with angularly dependent probability for light absorption in the *trans*-state.[4,37] Reorientation of *trans*-isomers out from polarization direction of the UV light produces a decrease of UV absorption and consequently the patterning process is less and less efficient.[38,39] This leads to the decrease of the diffraction efficiency. The effect is most profound in the "free" configuration, in which there is no constrains on rearrangements of the LCE film, while in the "constrained" and especially in the "clamped" configuration external strain hinders shrinking and hence also reorganization.

An interesting question that rises at this point is why photoinduced alignment appears to be negligible or at least much weaker in the SCE-p compound. The reason might be an anisotropic local molecular field associated with the liquid-crystalline order, which produces a torque that pushes the mesogenic *trans*-isomers back to the orientation along **n**. In the SCE-p material, this torque have no competing effects, while in the SCE-c material structural forces originating from the direct network shrinking seem to be prevailing and acting in favor of the photoinduced alignment.

3.2. Depth of Refractive Index Modulation

In kinetics experiments (Figure 4 and 5), diffraction efficiency was measured at normal incidence of the probe beam with respect to the sample surface. Due to this, one of the reasons for the decrease of the diffraction efficiency with prolonged UV exposures can also be the transition from a thin-grating (Raman-Nath) to a thick-grating (two-beam coupling) diffraction regime.[34] For the former diffraction efficiency does practically not dependent on the angle of incidence, while for the latter diffraction efficiency is only large for incidence at the Bragg angle $\alpha = \alpha_B$ and rapidly decreases with deviation from the Bragg angle. A variation of diffraction regime occurs due to the increasing depth of the patterning with UV illumination.

To resolve this issue, the angular dependence of the intensity of the +1st order diffraction peak (rocking-curve) was measured for different UV illumination times. The results, normalized to $I_{+1}(\alpha = 0) = 1$, are shown in Figure 6. The angle $\alpha = 0$ corresponds to normal incidence. The periodicity of the recorded grating structures was $\Lambda = 9.3$ μm. Therefore, the associated Bragg configuration angle is $\alpha_B = \arcsin(\lambda_P/2\Lambda) = 0.034$ rd. One can notice that even for long UV exposures the angular width σ_α (FWHM) of the diffraction peaks is considerably larger than α_B,

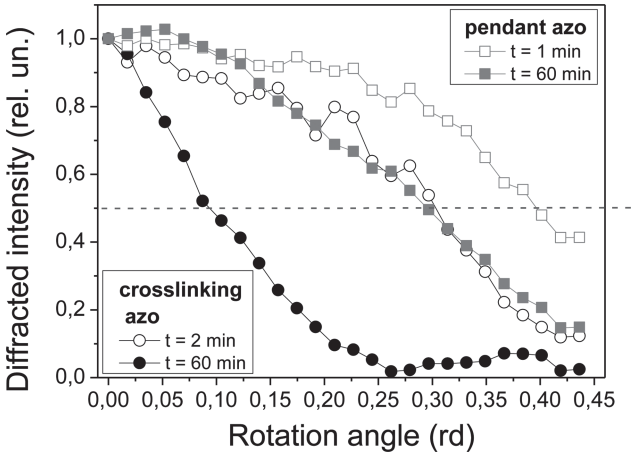

Figure 6. Angular dependence of the intensity of the +1st order diffraction peak for short (open symbols) and long (solid symbols) UV exposure times. The squares denote material with pendant azobenzene molecules (SCE-p) and the circles material with crosslinking azobenzene units (SCE-c).

which means that measurements performed at $\alpha = 0$ provide reasonable information on the refractive index modulation for all investigated UV illumination times.

As shown in our recent paper, the angular width of the diffraction peak can be used to deduce the effective depth of the recorded grating structure.[32] This depth is inversely proportional to the width of the diffraction peak. From the data shown in Figure 6, it follows that the depth of patterning is considerably larger in the SCE-c sample than in the SCE-p sample. This finding is in agreement with the above-discussed photoinduced alignment of *trans*-azobenzene molecules, which results in a decrease of absorption and hence a larger penetration depth. The effective thickness of the grating structure is given as $d_{eff} \approx (\Lambda/\sigma_\alpha)$, which gives $d_{eff} \approx 10$ μm for SCE-p after 1 min of UV illumination, $d_{eff} \approx 15$ μm for SCE-p after 60 min and for SCE-c after 2 min of UV illumination, and $d_{eff} \approx 45$ μm for SCE-c after 60 min of UV illumination. All values of d_{eff} are significantly smaller than the thickness (≈300 μm) of the LCE film. So a large part of the material structure remains unperturbed.

3.3. Angular Dependence of Refractive Index Modulation

LCEs are optically anisotropic materials. So the refractive index modulation produced by UV irradiation is expected to exhibit different diffraction properties for different polarization angles θ of the probe beam (Figure 3). Figure 7 shows obtained dependencies of $\eta(\theta)$ for the material with pendant azobenzene molecules (SCE-p). UV irradiation was terminated slightly after a maximum value of η for extraordinary polarized probe beam (θ = 90°) was observed (see Figure 4). Polarization direction of the probe beam was rotated for two full rotations in steps of 10°. A gradual decrease of the signal from the first to the last measured data point is a consequence of the spontaneous *cis*-to-*trans*-thermal back-isomerization process, which at room temperature exhibits a decay time of several hours. One can notice that for all mounting configurations the diffraction efficiency is about four times larger for extraordinary polarization (θ = 90°, e) than for ordinary polarization (θ = 0°, o).

Figure 8 shows the results of analogous measurements for sample SCE-c. The results are very similar as for the sample SCE-p. Also for SCE-c material, η is about four times larger for extraordinary polarization than for ordinary polarization. In the following, we will show that this can be explained by the intrinsic properties of the nematic phase.

The order parameter S of the nematic phase is related to the optical anisotropy of the LCE medium. The optical dielectric tensor is optically uniaxial with optical axis parallel to the director **n**. Its principal components $\varepsilon_{II} = (n_e)^2$ and $\varepsilon_\perp = (n_o)^2$ (where II and ⊥ denote directions parallel and perpendicular to **n,** and n_e and n_o denote extraordinary an ordinary refractive index, respectively) are related to the average dielectric constant $\bar{\varepsilon}$ and dielectric anisotropy ε_a as:[38,40]

$$\bar{\varepsilon} = \frac{2\varepsilon_\perp + \varepsilon_{II}}{3},\ \varepsilon_a = (\varepsilon_{II} - \varepsilon_\perp) \approx \beta S \qquad (4)$$

The proportionality constant β depends on the volume density of the mesogenic molecular units and the anisotropy of their molecular polarizability.

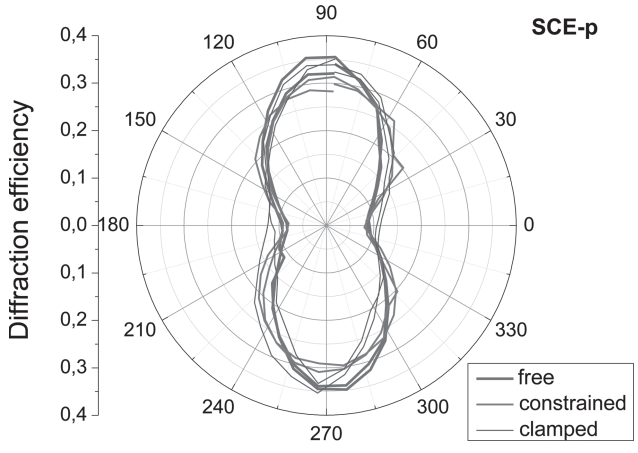

Figure 7. Dependence of the +1st order diffraction efficiency on polarization direction of the linearly polarized probe beam for material with pendant azobenzene units (SCE-p). The orientations θ = 0 correspond to ordinary (o) and θ = 90° to extraordinary (e) polarization, respectively. The different colours/line thicknesses correspond to different mounting arrangements of the sample.

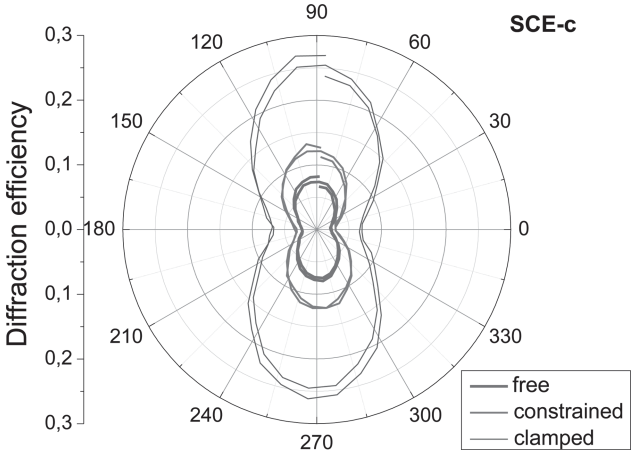

Figure 8. Dependence of the +1st order diffraction efficiency on polarization direction of the linearly polarized probe beam for material with crosslinking azobenzene units (SCE-c). Orientations θ = 0 correspond to ordinary (o) and θ = 90° to extraordinary (e) polarization, respectively. Different colours/line thicknesses correspond to different mounting arrangements of the sample.

According to Equation 4, any variation of order parameter S produces variations of ε_{II} and $\varepsilon_{\perp}$ given by

$$\Delta\varepsilon_{II} \approx \frac{2}{3}\beta\Delta S, \quad \Delta\varepsilon_{\perp} \approx -\frac{1}{3}\beta\Delta S \tag{5}$$

For small ΔS, it follows that:

$$\Delta n_e \approx \frac{1}{3}\beta\Delta S/n_e, \quad \Delta n_o \approx -\frac{1}{6}\beta\Delta S/n_o \tag{6}$$

In accordance with Equation 6, spatial variation of S induced by inhomogeneous UV illumination produces spatial modulation of both the extraordinary and the ordinary refractive index of the LCE. The modulations have opposite phase and the modulation amplitude for extraordinary polarization is about two times larger than the modulation amplitude for ordinary polarization.

For small modulation amplitudes, the diffraction efficiency of the grating structure η is proportional to the square of the modulation amplitude Δn,[34] from which one obtains:

$$\frac{\eta_e}{\eta_o} = \left(2\frac{n_o}{n_e}\right)^2 \approx 4 \tag{7}$$

This result is in very good agreement with our observations. To describe the complete dependence of η on θ, one should decompose the incident polarization vector $\mathbf{E}_{in}$ into its extraordinary and ordinary components:

$$\mathbf{E}_{in} = E_0\left(\mathbf{e}_o\cos\theta + \mathbf{e}_e\sin\theta\right) \tag{8}$$

where $\mathbf{e}_o$ and $\mathbf{e}_e$ are unit vectors perpendicular and parallel to the nematic director $\mathbf{n}$. The corresponding diffraction efficiency is then given by:

$$\eta \propto \left(\Delta n_o\cos\theta\right)^2 + \left(\Delta n_e\sin\theta\right)^2 \approx C\left[(\cos\theta)^2 + 4(\sin\theta)^2\right] \tag{9}$$

The fit of Equation 9 to the experimentally obtained dependence of $\eta(\theta)$ for the "clamped" sample of the SCE-c is shown in Figure 9. The agreement between data and theory is very good. From this result, we conclude that UV irradiation-induced refractive index modulation in the LCE materials can be well described by considering only the bulk response of the nematic phase. This indicates that a contribution from the UV-irradiation-induced surface relief structure is negligible. Surface relief gratings usually play a very important role in photosensitive polymeric materials at temperatures below the glass transition temperature T_g, however, all our measurements were performed at $T > T_g$ where this effect is usually absent.[1]

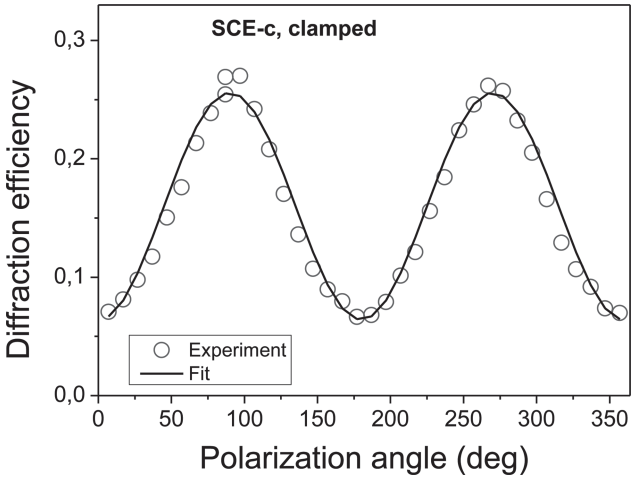

Figure 9. Dependence of the +1st order diffraction efficiency on polarization direction of the linearly polarized probe beam for material with crosslinking azobenzene units in clamped configuration. Orientations $\theta = 0$ correspond to ordinary (o) and $\theta = 90°$ to extraordinary (e) polarization, respectively. Solid line is a fit to Equation 9.

4. Conclusion

Our observations demonstrate that the way of incorporation of azobenzene derivatives into the LCE matrix strongly affects optical-patterning capability of the material. We observed that UV-irradiation-induced variation of refractive index is significantly larger in the material with pendant azobenzene molecules than in the material with crosslinking azobenzene units. This signifies that chemical attachment of the mesogenic azobenzene-units as pendant groups leads to their optimal compatibility with the nematic phase. This provides large localized modifications of the nematic- order parameter and correspondingly also large localized modification of optical birefringence of the medium. UV illumination of the same type of LCE with azoderivatives attached as crosslinking units produces more delocalized illumination-induced perturbations and consequently the refractive index modulation is smaller.

The observed dependence of optical diffraction properties on polarization state of the probe beam resolves that UV-irradiation-induced refractive index modulation is practically entirely of the bulk origin. This abandons the often proposed hint that surface undulation gratings should play an important role in the light-induced microstructuring of LCE films. This is explained by the fact that the glass transition temperatures of conventional

polysiloxane-based LCE materials are usually below the typical temperatures used for their investigations.

Large differences in the kinetics of UV-irradiation-induced changes between both investigated materials suggest that also photoinduced alignment of the azobenzene groups strongly depends on the way of their incorporation into the LCE structure. The alignment effect seems to be very strong for azobenzene units that are built into the structure as crosslinkers, while it appears to be practically negligible for pendant azobenzene moieties. Anyhow, as our experiments provide only indirect evidence, further experiments are needed to fully resolve the issue of photoinduced alignment in LCE materials.

Acknowledgements: We gratefully acknowledge financial support in the frame of the Slovenian research program P1–0192 – "Light and Matter" and the International S&T cooperation program of China 2011DFA52870 – "Cooperative research on novel photosensitive polymeric nanocomposites and their photonic microstructures".

Received: July 26, 2013; Revised: August 30, 2013; Published online: October 7, 2013; DOI: 10.1002/macp.201300493

Keywords: holographic lithography; liquid crystal elastomers; optical diffraction gratings; optical patterning; photosensitive materials

[1] Y. Zhao, T. Ikeda, *Smart Light Responsive Materials – Azobenzene-Containing Polymers and Liquid Crystals*, Wiley, Hoboken, NJ, USA **2009**.
[2] J. Ryu, M. D'Amato, X. Cui, K. N. Long, H. J. Qi, *Appl. Phys. Lett.* **2013**, *100*, 161908.
[3] A. Natansohn, P. Rochon, *Chem. Rev.* **2002**, *102*, 4139.
[4] P. J. Shannon, W. M. Gibbons, S. T. Sun, B. J. Swetlin, *Nature* **1991**, *351*, 49.
[5] M. Warner, E. M. Terentjev, *Liquid Crystal Elastomers*, Oxford University Press, New York, USA **2007**.
[6] H. Finkelmann, E. Nishikawa, G. G. Pereira, M. Warner, *Phys. Rev. Lett.* **2001**, *87*, 015501.
[7] D. Corbett, M. Warner, *Liq. Cryst.* **2009**, *36*, 1263.
[8] P. M. Hogan, A. R. Tajbakhsh, E. M. Terentjev, *Phys. Rev. E* **2002**, *65*, 041720.
[9] Y. L. Yu, M. Nakano, T. Ikeda, *Nature* **2003**, *425*, 145.
[10] M. Warner, L. Mahadevan, *Phys. Rev. Lett.* **2004**, *92*, 134302.
[11] N. J. Dawson, M. G. Kuzyk, J. Neal, P. Luchette, P. Palffy-Muhoray, *J. Opt. Soc. Am. B* **2011**, *28*, 1916.
[12] H. Y. Jiang, S. Kelch, A. Lendlein, *Adv. Mater.* **2006**, *18*, 1471.
[13] U. Hrozhyk, S. Serak, N. Tabiryan, T. J. White, T. J. Bunning, *Opt. Express* **2009**, *17*, 716.
[14] K. M. Lee, M. L. Smith, H. Koerner, N. Tabiryan, R. A. Vaia, T. J. Bunning, T. J. White, *Adv. Funct. Mater.* **2011**, *21*, 2913.
[15] M. Camacho-Lopez, H. Finkelmann, P. Palffy-Muhoray, M. Shelley, *Nat. Mater.* **2004**, *3*, 307.
[16] J. Cviklinski, A. R. Tajbakhsh, E. M. Terentjev, *Eur. Phys. J. E* **2002**, *9*, 427.
[17] C. L. M. Harvey, E. M. Terentjev, *Eur. Phys. J. E* **2007**, *23*, 185.
[18] A. Sanchez-Ferrer, *Proc. SPIE* **2011**, *8107*, 810702.
[19] M. H. Li, P. Keller, B. Li, X. Wang, M. Brunet, *Adv. Mater.* **2003**, *15*, 569.
[20] C. L. van Osten, C. W. M. Bastiaansen, D. J. Broer, *Nat. Mater.* **2009**, *8*, 677.
[21] S. V. Serak, N. V. Tabiryan, T. J. White, T. J. Bunning, *Opt. Express* **2009**, *17*, 15736.
[22] M. H. Li, P. Keller, *Philos. Trans. R. Soc. A* **2006**, *364*, 2763.
[23] C. Ohm, M. Brehmer, R. Zentel, *Adv. Mater.* **2010**, *22*, 3366.
[24] E. Sungur, M. H. Li, G. Taupier, A. Boeglin, M. Romeo, S. Mery, P. Keller, K. D. Dorkenoo, *Opt. Express* **2007**, *15*, 6784.
[25] M. Devetak, B. Zupancič, A. Lebar, P. Umek, B. Zalar, V. Domenici, G. Ambrožič, M. Žigon, M. Čopič, I. Drevenšek-Olenik, *Phys. Rev. E* **2009**, *80*, 050701.
[26] M. Gregorc, H. Li, V. Domenici, I. Drevensek Olenik, *Proc. SPIE* **2012**, *8556*, 855616.
[27] W. H. de Jeu, *Liquid Crystal Elastomers: Materials and Applications*, Springer Verlag, Berlin, Heidelberg, Germany **2012**.
[28] A. Sánchez-Ferrer, A. Merekalov, H. Finkelmann, *Macromol. Rapid Commun.* **2011**, *32*, 671.
[29] A. Sánchez-Ferrer, H. Finkelmann, *Soft Matter* **2013**, *9*, 4621.
[30] J. Kupfer, H. Finkelmann, *Makromol. Chem. Rapid Commun.* **1991**, *12*, 717.
[31] M. Gregorc, H. Li, V. Domenici, G. Ambrožič, M. Čopič, I. Drevenšek-Olenik, *Materials* **2012**, *5*, 741.
[32] M. Gregorc, B. Zalar, V. Domenici, G. Ambrožič, I. Drevenšek-Olenik, M. Fally, M. Čopič, *Phys. Rev. E* **2011**, *84*, 031707.
[33] M. Knežević, M. Warner, M. Čopič, A. Sánchez-Ferrer, *Phys. Rev. E* **2013**, *87*, 062503.
[34] P. Hariharan, *Optical Holography: Principles, Techniques, and Applications*, 2nd ed., Cambridge University Press, New York **1996**.
[35] M. Gregorc, H. Li, V. Domenici, G. Ambrožič, M. Čopič, I. Drevenšek-Olenik, *Phys. Rev E* **2013**, *87*, 022507.
[36] J. Garcia-Amoros, H. Finkelmann, D. Valasco, *J. Mater. Chem.* **2011**, *21*, 1094.
[37] I. Janossy, *Phys. Rev. E* **1994**, *49*, 2957.
[38] J. Chen, D. L. Johnson, P. J. Boss, X. Wang, J. L. West, *Phys. Rev. E* **1996**, *54*, 1599.
[39] H. G. Galabova, D. W. Allender, J. Chen, *Phys. Rev. E* **1997**, *55*, 1672.
[40] G. Barbero, L. R. Evangelista, *An Elementary Course on Continuum Theory for Nematic Liquid Crystals*, Word Scientific, Singapore **2001**.